

Compensation for the azimuthal anisotropy of PS-converted waves in HTI media

Weining Liu, Hengchang Dai, and Xiang-Yang Li, British Geological Survey,

This paper studies the azimuthal anisotropy of PS-converted waves recorded in the horizontal radial and transverse components in HTI media. Due to converted wave splitting, the horizontal radial and transverse components contain two types of converted wave: the fast P-SV1 and the slow P-SV2 that propagate along the directions parallel and perpendicular to the fracture strike, respectively. The NMO velocity variations of both the P-SV1 and P-SV2 waves are close to two different ellipses. Therefore it is necessary to analyse and compensate individually for the azimuthal anisotropy of each of the P-SV1 and P-SV2 waves. By applying two NMO-velocity ellipses to the synthetic and field data, the NMO correction results are improved.

Introduction

The presence of natural fractures affects the fluid flow in hydrocarbon reservoirs and provides potential pathways for hydrocarbon migration. As a result, fracture detection and characterisation has become increasingly important for hydrocarbon exploration. Assuming vertically aligned fractures give rise to transverse isotropy with a horizontal symmetry axis (or HTI), fracture properties can be inverted from the seismic reflection data. Compensating for the azimuthal anisotropy induced by vertical fractures can improve the imaging of subsurface structures.

P-wave azimuthal anisotropy is intensely studied and several methods are proposed to measure it (Rüger, 1996; Tsvankin, 1997; Li, et al., 2003). Compared with the P-wave, shear-waves are more sensitive to the azimuthal anisotropy induced by fractures, whilst the PS converted wave which retains the behaviour of both P- and S-waves, is more efficient for characterising the fractured reservoir. Current studies often focus on the use of converted-wave splitting for fracture detection (e.g. Simmons, 2009; Cheng et al., 2009). There are a few studies on the use of the azimuthal behaviour of PS converted waves recorded in radial component data (Mattocks et al., 2005; Dai, 2010).

In this paper, we analyse the azimuthal behaviour of the PS converted-wave and its effect on converted-wave splitting. Full-wave synthetics are used to show the azimuthal behaviour and the splitting of converted-waves in the HTI media induced by vertical fractures. The modelling result shows that the splitting should be compensated for, before the azimuthal behaviour is analyzed. This approach is applied to field data acquired in Daqing, China. The results obtained from both synthetic and field data show that the converted-wave splitting has to be accounted for, before the azimuthal variation can be revealed.

Theory

In a converted-wave survey, the P-SV mode wave that is polarised in the radial direction is considered as the primary PS converted wave (Figure 1). In HTI media, it splits into a fast (P-SV1) and a slow converted wave (P-SV2). P-SV1 is polarised in the fracture direction (the isotropy plane) and P-SV2 is polarised parallel to the fracture normal (in the plane containing the symmetry-axis). Note that for propagation in the azimuthal plane parallel to the fracture direction, shear-wave splitting does not occur in this direction, when only the P-SV1 wave is observed, and in the direction perpendicular to the fracture strike, when only the P-SV2 wave is observed. For other azimuths, both P-SV1 waves and P-SV2 waves are projected into the radial component with the consistent polarisations and the transverse component with polarity reversals every 90 degrees.

Both the P-SV1 wave and P-SV2 wave are affected by the azimuthal anisotropy. Some attributes of the P-SV1 wave and the P-SV2 wave vary azimuthally, which is similar to the variation of the attributes of the pure-mode waves. Specifically, the NMO velocity of the P-SV1 wave reaches its maximum and minimum in the direction parallel and perpendicular to the fracture direction respectively. In contrast, the maximum and minimum of the NMO velocity of the P-SV2 wave appear in the direction perpendicular and parallel to the fracture direction respectively. Furthermore, in weakly anisotropic media, the differences of the maximum and minimum of the NMO velocities are relatively small. Therefore the NMO velocities of both the P-SV1 wave and P-SV2 wave can be represented by elliptical variations in the azimuthal plane, which can be expressed:

$$v_{1-nmo}^2(\theta) \approx v_1^2 + \Delta_1^2 \cos(2\theta) \quad (1) \quad v_{2-nmo}^2(\theta) \approx v_2^2 + \Delta_2^2 \cos(2\theta) \quad (2)$$

where v_{1-nmo} and v_{2-nmo} are the NMO velocities of the P-SV1 wave and P-SV2 wave respectively.

$v_1^2 = (v_{1-nmo-max}^2 + v_{1-nmo-min}^2) / 2$, $v_2^2 = (v_{2-nmo-max}^2 + v_{2-nmo-min}^2) / 2$; $\Delta_1^2 = (v_{1-nmo-max}^2 - v_{1-nmo-min}^2) / 2$, $\Delta_2^2 = (v_{2-nmo-max}^2 - v_{2-nmo-min}^2) / 2$, where $v_{1-nmo-max}$ and $v_{1-nmo-min}$ are the maximum and minimum values of the NMO velocity of the P-SV1, and $v_{2-nmo-max}$ and $v_{2-nmo-min}$ are the maximum and

minimum values of the NMO velocity of P-SV2. θ is the azimuthal angle between the vertical plane and the fracture direction.

Therefore, in HTI media, in order to analyse and compensate for the azimuthal variation of the PS converted wave recorded in the radial component, it is essential to consider the P-SV1 and P-SV2 waves separately because their NMO velocities vary differently in the azimuthal plane. By horizontal rotation of the radial and transverse component, the P-SV1 and P-SV2 component can be obtained. Then the NMO velocity ellipses for both P-SV1 and P-SV2 are calculated by the velocity analysis of different azimuth gathers, which can improve the NMO correction results for both the P-SV1 and P-SV2 components.

Synthetic study

In this study, a synthetic dataset is generated by the reflectivity method (Taylor, 2001). Figure 2 shows this model which contains three layers and the parameters of each layer. The top layer is an isotropic layer and the middle layer is a HTI layer that is induced by vertically aligned fractures. The bottom layer is the isotropic halfspace. The fracture density is 0.1 in the HTI layer and the fracture strike is 120° in the azimuthal plane (Figure 1). The offset range of this dataset is from 500m to 1500m; the azimuth range is from 0° to 360° with the interval being 2° .

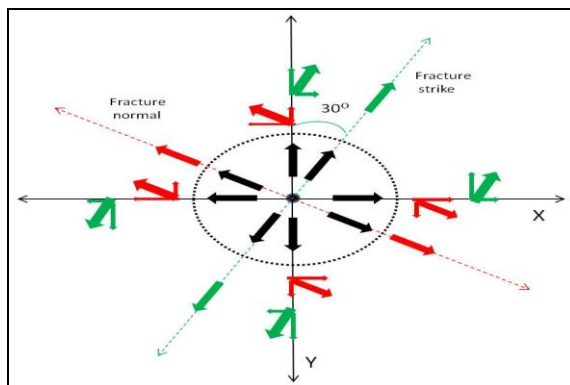


Figure 1.

Isotropic	$v_p = 1400\text{m/s}, v_s = 400\text{m/s},$ $\rho = 1.1\text{g/cm}^3 \Delta z = 700\text{m}$
HTI	$v_p = 1500\text{m/s}, v_s = 700\text{m/s},$ $\rho = 1.2\text{g/cm}^3 \Delta z = 300\text{m}$
Isotropic halfspace	$v_p = 1900\text{m/s}, v_s = 900\text{m/s},$ $\rho = 1.3\text{g/cm}^3$

Figure 2.

Figure 1: the source is at the centre point whilst the receivers are azimuthally placed (black dotted circle, offset 1000m). The fracture strike is 120° in the azimuthal plane. The P-SV wave (black arrows) is oriented in the radial component and splits into the fast P-SV1 wave (green arrows) and the slow P-SV2 wave (red arrows). The P-SV1 and P-SV2 waves are oriented in the directions parallel and perpendicular to the fracture strike, respectively, and are both projected into the radial component with the consistent polarity and the transverse component with the opposite polarities. In the direction parallel to the fracture strike, only the P-SV1 wave is observed. In the direction perpendicular to the fracture strike, only the P-SV2 wave is observed.

Figure 2: The parameters of the model. The fracture strike is 120° in the azimuthal plane.

The azimuth gathers (offset 1000m) of the radial, transverse and vertical components are shown in Figure 3. The red ellipses emphasise the target event that is affected by the HTI layer. Figure 4 is the enlargement of the red ellipses in Figure 3. Note that the fast P-SV1 wave and slow P-SV2 wave are observed in both the radial (Figure 4(a)) and transverse (Figure 4(b)) component but with different patterns of azimuthal variation. Furthermore the azimuthal anisotropy of the P-wave recorded in the vertical component is similar to that of the P-SV1 wave, but it is less significant than that of the P-SV1 wave. The fast directions for P-SV1 (red arrows in Figure 4(a)) and P-SV2 (blue arrows in Figure 4(b)) are along the directions parallel and perpendicular to the fracture strike respectively. Therefore it is inaccurate to consider the PS converted waves observed in the radial component as a single type of converted wave. If the fracture direction is known, the radial and transverse component data can be rotated into the fast direction that contains only the P-SV1 wave, and the slow direction that only contains the P-SV2 wave. The azimuthal variations shown in the P-SV1 wave (Figure 5(a)) and P-SV2 wave (Figure 5(b)) are much clearer than the data in the radial and transverse components.

Once the split shear-waves are separated, azimuthal velocity analysis can be applied to the P-SV1 and P-SV2 waves and the different velocity ellipses are fitted into Equations (1) and (2). The NMO correction results for both the P-SV1 wave and P-SV2 wave are shown in Figure 6. The events in both Figure 6(a) and 6(c) are better-corrected by applying the velocity ellipse.

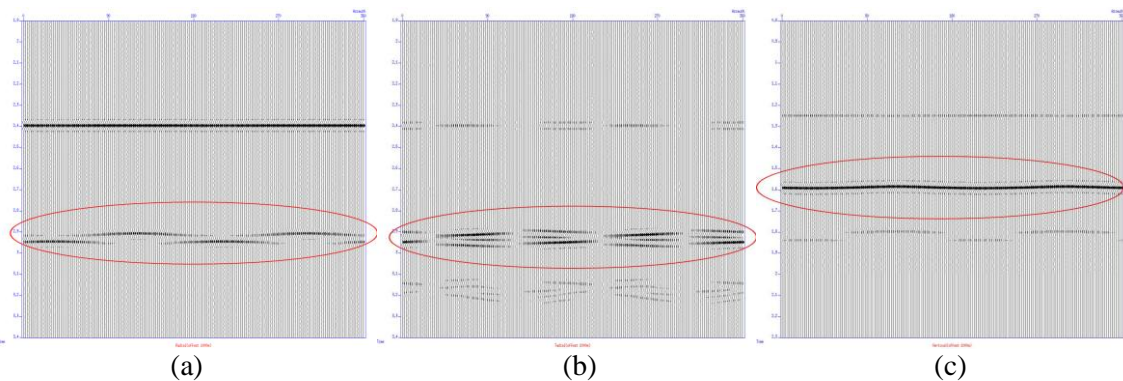


Figure 3: the azimuth gathers (offset 1000m) of the (a) radial, (b) transverse, and (c) vertical components.

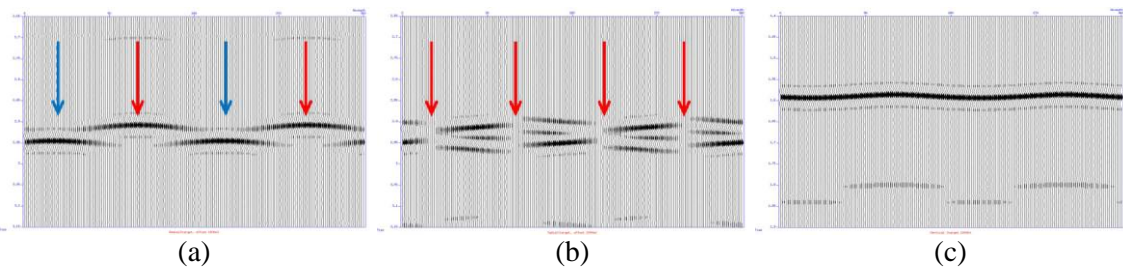


Figure 4: The enlargements of the target event in the (a) radial, (b) transverse, and (c) vertical components

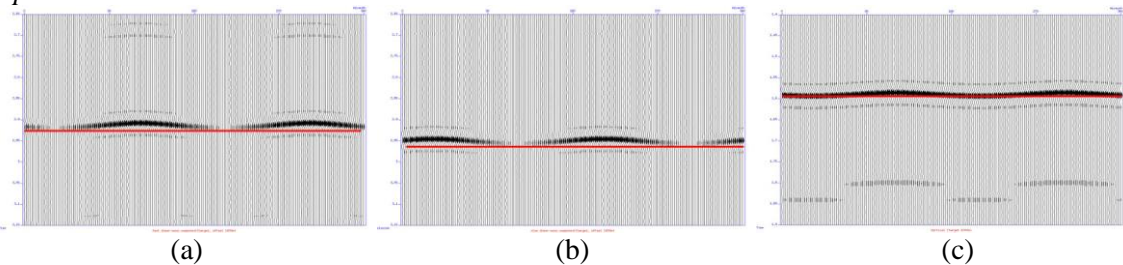


Figure 5: The azimuth gathers (offset 1000m) of the target events in the (a) fast P-SV1 and (b) slow P-SV2 components, and in (c) the vertical component.

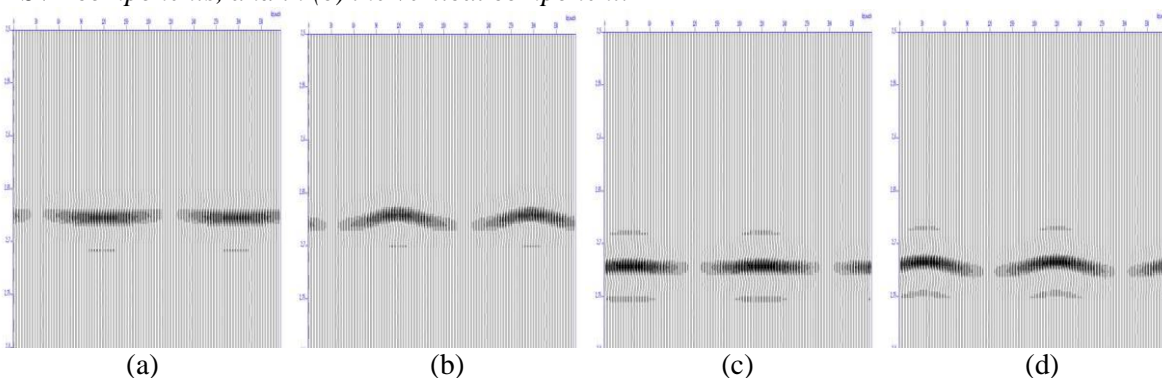


Figure 6: The NMO correction results at the offset (1000m) for the P-SV1 wave ((a): with the velocity ellipse, (b): without the velocity ellipse) and the P-SV2 wave ((a): with the velocity ellipse, (b): without the velocity ellipse).

Field data

This analysis procedure is also applied to a land 3D dataset acquired in Daqing Oil field that is located in the northeast of China. The NMO correction results for a super-CDP gather of the P-SV1 wave are shown in Figure 7. By considering the P-SV1 wave individually and applying the velocity ellipse (Equation (1)), the events in Figure 7c are flatter and better focused.

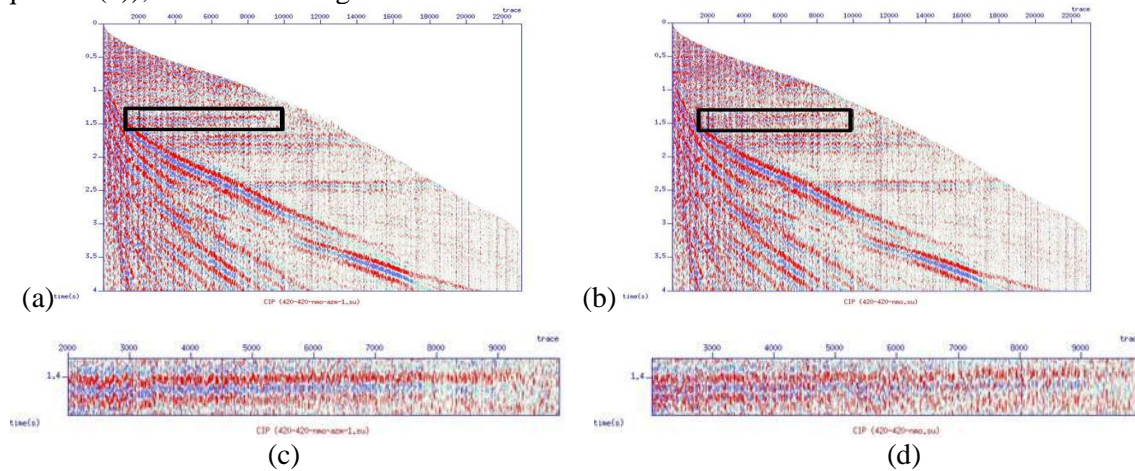


Figure 7: The NMO correction results for a super-CDP gather of the P-SV1 wave ((a): with the velocity ellipse, (b): without the velocity ellipse, (c) and (d) are the enlarged black rectangles of (a) and (b) respectively).

Conclusion

This theoretical and synthetic study has showed that the azimuthal behaviour of the PS-converted wave in fracture-induced HTI media is complicated by the phenomenon of shear-wave splitting. The split shear-waves (fast P-SV1 and slow P-SV2) have to be separated first before compensating for the azimuthal variations. The variation of NMO velocity of both P-SV1 and P-SV2 waves is close to an ellipse. By applying the velocity ellipse, the NMO correction of both synthetic and field data are improved.

Acknowledgements

This work is supported by the Edinburgh Anisotropy Project (EAP) of the British Geological Survey, and is published with the permission of the Executive Director of the British Geological Survey (NERC) and the EAP sponsors

References

- Cheng, B., Xu, T. and Tang, J., 2009, Splitting estimation and compensation of converted wave in multilayer fracture media: A numerical modelling study. CPS/SEG Beijing 2009 International Geophysical Conference & Exploration.
- Dai, H., Li, X-Y., Yu, C. and Wang, J., 2010, A practical approach to compensate for the azimuth anisotropy in 3D PS converted wave processing, 72nd EAGE annual meeting, 14-17.
- Li, X., Liu, Y., Liu, E., Shen, F., Li, Q., Qu, S., 2003, Fracture detection using land 3D seismic data from the Yellow River data, China, The Leading Edge, July 2003, 680-683;
- Mattocks, B., Li, J. and Roche, S., 2005, Converted-wave azimuthal anisotropy in a carbonate foreland basin, 75th SEG Meeting, Expanded Abstracts, 24, 897.
- Rüger A. 1996, Variation of P-wave reflectivity with offset and azimuth in anisotropic media. 66th SEG Meeting, Expanded Abstracts, 1810-1813.
- Simmons, J., 2009, converted-wave splitting estimation and compensation, Geophysics, 74, D37.
- Taylor, D.B., 2001, Manual: Version 5.5 Macro Ltd, 31 Palmerston Place, Edinburgh.
- Tsvankin, I., 1997, Reflection moveout and parameter estimation for horizontal transverse isotropy, Geophysics, 62, 2, 614-629